International Journal of GEOMATE, March., 2021, Vol.20, Issue 79, pp. 161-167
ISSN: 2186-2982 (P), 2186-2990 (O), Japan, DOI: https://doi.org/10.21660/2021.79.j2042
Geotechnique, Construction Materials and Environment

IMPROVING FLEXURAL MOMENT CAPACITY OF CONCRETE BEAM BY CHANGING THE REINFORCEMENT CONFIGURATION

*Hamkah[1], Pieter Lourens Frans[2], and Zubair Saing[3]

[1, 2] Department of Civil Engineering, Politeknik Negeri Ambon, Indonesia
[3]Department of Civil Engineering, Universitas Muhammadiyah Maluku Utara, Ternate, Indonesia

*Corresponding Author, Received: 30 Nov. 2020, Revised: 28 Dec. 2020, Accepted: 21 Jan. 2021

ABSTRACT: The bar used for concrete beams is generally in shear or stirrups mounted perpendicular to the beam axis. The idea underlying this problem arises from the observation of reinforced concrete beams by changing the configuration of vertical shear reinforcement to less sloping reinforcement, which would be less relevant to the theory of its use. This study aims to analyze the skeletal system bending moment capacity reinforcing beams and producing a theoretical equation of the bending moment of reinforcing the skeletal system. This study is an experimental laboratory with twelve specimens consisting of three normal beams (BN) as control variable beams and nine frame reinforcement beams (BTR) as independent variables. Data were analyzed using the strength design method. The results showed that used reinforcement frame system increases the beam strength when it reaches the ultimate load on the flexural capacity with the MPF frame retaining moment on the BTR25 beam of 10.23%, the BTR50 beam of 7.47%, and the BTR75 beam of 4.60% of the beam BN and found the equation for calculated the frame retaining moment (MPF). The equation can be used for practical calculations of the retaining beam frame system (BTR).

Keywords: Moment capacity, Reinforcement frame system

1. INTRODUCTION

Different approaches have been developed in recent decades to improve the bending strength or rigidity of reinforced concrete beams. These techniques focus on increasing the flexural strength or rigidity of concrete beams by altering the reinforcement system configuration or adding additional aids in the beam bending area. This approach also results in higher costs and time and extra efforts.

Assume that the reinforcement device within the concrete beam can provide greater flexural strength without altering the reinforcement geometry or using additional tools where bending takes place. In that case, the use of traditional approaches would be economical and also convenient. To improve the RC beams flexural ability, several researchers suggest the use of inclined shear reinforcement. The inclined stirrup beams exhibit final strength but less deflection than the vertical and horizontal bar systems [1-3]. A tension bar at the bottom and a compression bar at the top are the Truss structure of the beam. Due to the diagonal bars strut action linking the horizontal bars on the upper cord and bottom cord, the coupling arm between the tension force and the compression force occurs in maintaining flexural action.

Recently in the construction industry, a special steel-concrete composite beam called Hybrid Steel Trussed Concrete Beams (HSTCBs) was introduced, in which prefabricated truss reinforcement is embedded within the concrete [4-6]. HSTCBs reflect a composite beam structural topology usually used as a significant structural solution consisting of a prefabricated steel truss embedded in a cast in situ concrete matrix. The truss structure is commonly built with and without a steel plate and a precast concrete slab in the HSTCBs, reflecting the bottom chord. Figure 1 illustrates a standard HSTCB.

HSTCBs load-carrying capacity is considered more than that of standard RC beams [7-10]. In this regard, this research examines the impact of truss system reinforcement on the flexural actions of reinforced concrete beams [11-14]. The load applied, the stress on the concrete compressive regions, the tensile steel in the mid-span, and the mid-span deflection were measured during the test up to failure [15]. The beam reactions were observed, and the effect of configuration was evaluated on deflections, strains, load power, crack patterns and mode of failure.

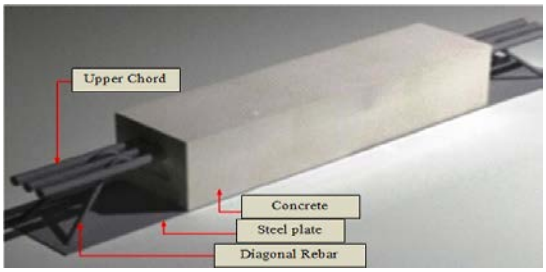

Fig. 1 Hybrid steel truss concrete beam [2]

2. MATERIALS AND METHODS

2.1 Specimens

In two stages, specimens were prepared: the truss reinforcements and the casting of the concrete beams. The specimen concrete beams measurements are 3300 mm long, with a width of 150 mm and a cross-section height of 200 mm. The descriptions of this specimen are shown in Fig. 2. Three beams of standard reinforced concrete (BN) and nine beams of truss reinforcement (BTR) were the specimens prepared in this analysis. There were 0.25d (BTR25), 0.5d (BTR50), and 0.75d (BTR75) space diagonal bars on the truss reinforcement, as shown in Fig. 3.

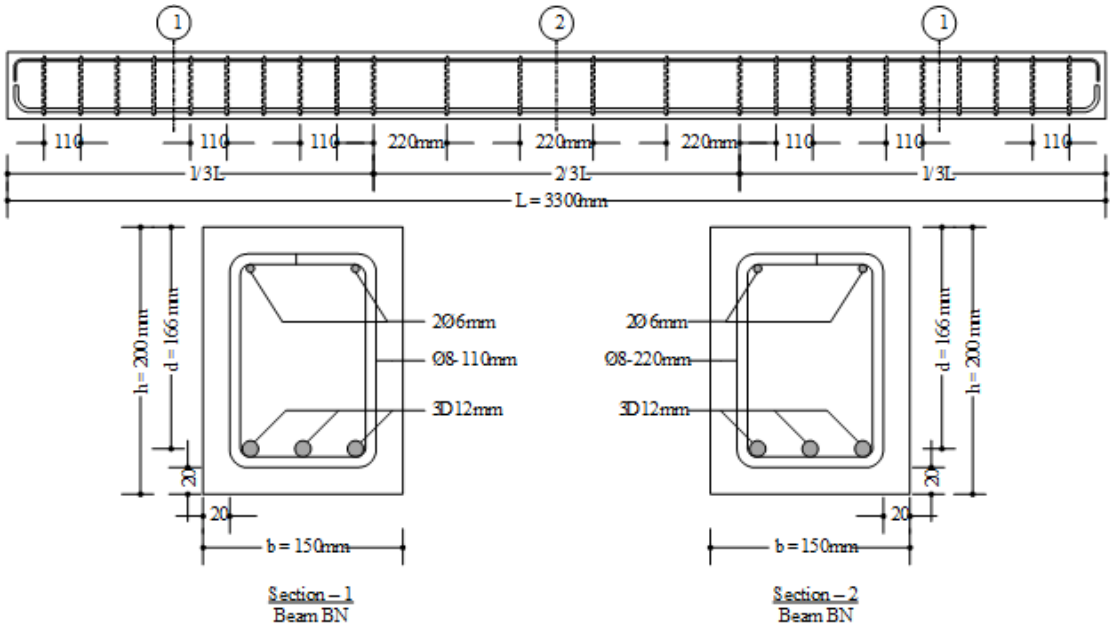

Fig. 2 Beam type BN

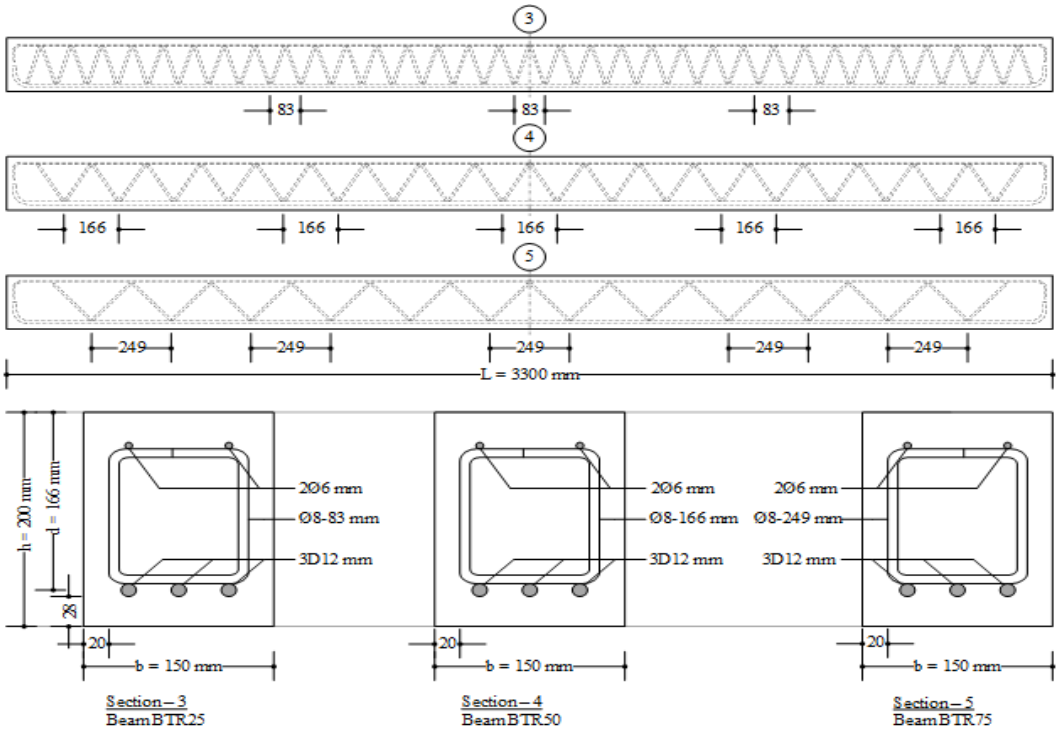

Fig. 3 Beam type BTR

Three of the D12 steel bars were used by Specimens BN as tensile reinforcement and D8 as the (vertical) shear reinforcement. On the compression side, BN had two D6 steel reinforcements for reinforcement assembly purposes only. The truss reinforcement was made of three D12 steel reinforcement bars for tension reinforcement, D8 steel reinforcement bars for diagonal bars, and two D6 steel reinforcement bars on the upper horizontal bars for BTR. All links were performed by welding in the truss reinforcement. The preparation of beam samples can be seen in Figures 2 and 3. In the moisturizing state, all specimens were cured for 28 days before testing. Table 1 presents the material properties of the reinforcement of concrete and steel used in this analysis.

2.2 Test Setup

At the three points at the middle of the span, one at the top of the beam and two at the concrete web, strain gauges were patched on the concrete surface before the test and patched strain gauges on the concrete wall. The pressure for further analysis calculated the tension and diagonal bar were linked to a data logger. The supporters were prepared to serve as support for the hinge-roller. The specimens were loaded under a four-point bending examination, with a space of 2500 mm of specimen support. With 500 mm of space, two loading points were applied to the middle of the beams' span.

The specimen setup is presented in Fig. 4. The load was applied by mounting a hydraulic jack on a steel contrast frame firmly attached to the laboratory floor. The jack is controlled by a hydraulic control unit that imposes a specified displacement of 0.2 mm/sec. A load cell with a 200 kN capacity was placed between the jack and the distribution beam to measure the force applied correctly. LVDTs were installed on the center point and both under loading points to measure the deflection. All data were recorded using a data logger connected to the computer.

Table 1 Material properties

Concrete		Steel Reinforcement	
Compressive strength	18.50 MPa	Yield strength D12	304 MPa
Young Modulus	20 GPa	Yield strength D8	417 MPa
Poisson Ratio	0.2	Yield strength D6	440 MPa
Density	2.3 t/m^3	Theoretical upper limit	0.5

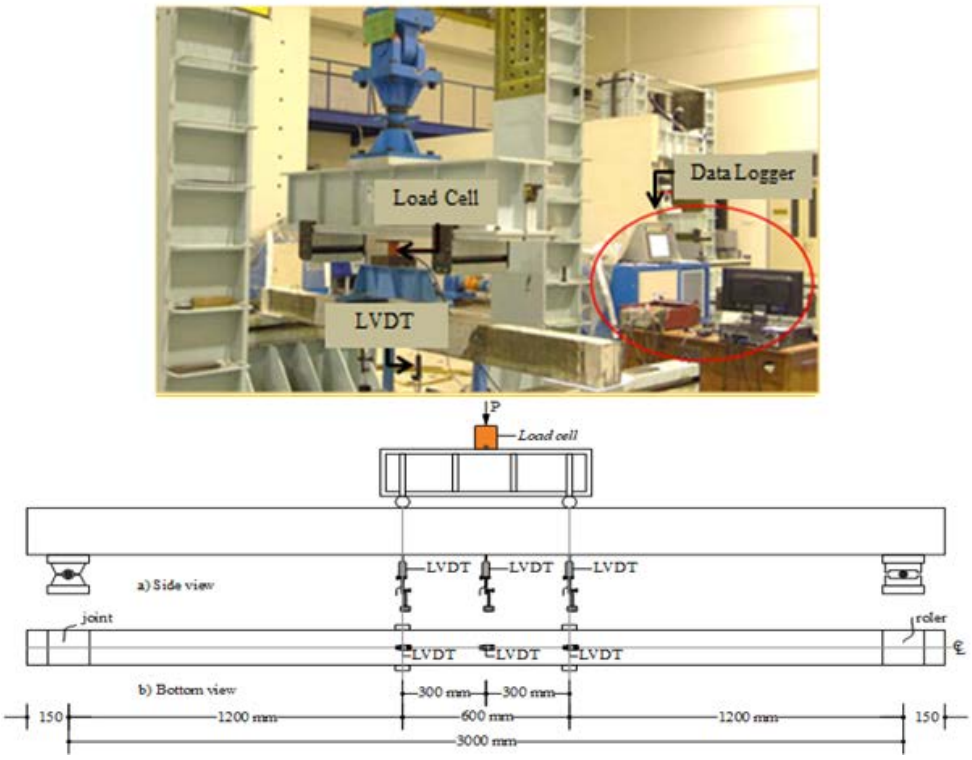

Fig. 4 Test setup

3. RESULTS AND DISCUSSIONS

3.1 Bending Moment Capacity

The beam deflection based on this test is determined at t time to be a momentary deflection under a bending moment M. The load has risen until there is a bending collapse. The deflection load test results show that the beam bends concerning the BN beam to the ultimate Pu load limit on the BTR25, BTR50, and BTR75 beams. The study results show that maximum deflection occurs in the middle of the period when the beam is loaded up to the final Pu load limit, with the deflection size varying according to the magnitude of the cross-section stiffness for BN beams and BTR beams [7, 10-12]. Table 2 shows the analysis of the bending moment capacity obtained by the additional capacity of the ultimate Pu load on the BTR25 beam increased by 10.72%, the BTR50 beam increased by 7.83%, and the BTR75 beam increased by 4.82% the BN beam.

According to space variations, the increase in failure load due to the geometric changes of vertical to diagonal stirrups reinforces the longitudinal tensile reinforcement as the substitute concrete (nAs) field. In addition, Pu load makes the stiffness of the BTR beam more rigid with more substantial ultimate moment potential than the BN beam based on the additional ultimate load capacity [1, 12, 15]. The increase of moment power in BN beams and BTR beams is shown in Figure 5. The Mu percentage on the BTR25 beam (10.23%), the BTR50 beam (7.47%), and the BTR75 beam (4.60%) from the BN beam were calculated for additional results.

3.2 Validation

The truss moment theoretical calculation is performed with a specific static engineering approach, which, when axially loaded, experiences rod extension, as shown in Fig. 6. Balance of the F and N horizontal rod powers, as in Equation 1.

Calculation of BTR beam retaining moment is done by Whitney's quadrilateral equivalent stress block theory approach. The assumption of compression stress is distributed at 0.85f'c. Evenly distributed in the equivalent compression region bounded by a straight line cross-section edge parallel to the neutral axis along a = β1.c of the fiber concrete experiences a maximum stress-strain εc [8, 9, 12, 15-18]. Based on Indonesian National Standards (SNI) 2847-2013, article 10 gives the value β1 = 0.85. With the force balance approach, T = C is shown in Figure 7.

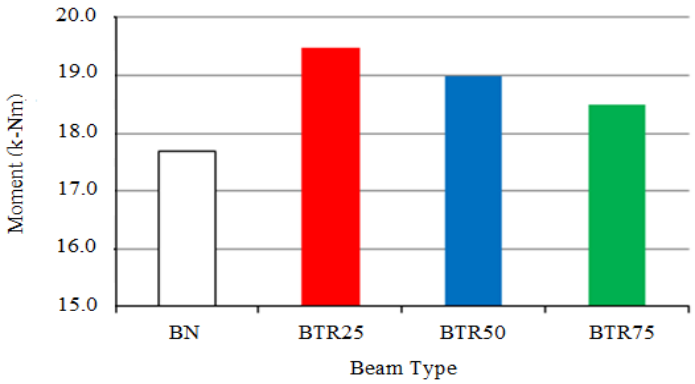

Fig.5 Percentage of your ultimate moment

Table 2 Percentage of ultimate moment

Specimen	Test results		Percentage	
	P_u (kN)	M_u (kNm)	P_u (%)	M_u (%)
Beam BN	28.11	17.67	-	-
Beam BTR25	31.12	19.48	10.72	10.23
Beam BTR50	30.31	18.99	7.83	7.47
Beam BTR75	29.46	18.49	4.82	4.60

$$\mathbf{F = N = \frac{P}{2\sin\emptyset} + \frac{P}{2} = \frac{P}{4\sin\emptyset}} \quad (1)$$

Where extension of the stem δ:

$$\mathbf{\delta_1 = \frac{F.L}{EA} = \frac{\frac{P}{4\sin\emptyset}\times h.\tan\emptyset}{EA} = \frac{Ph.\tan\emptyset}{EA.4\sin\emptyset}} \quad (2)$$

$$\mathbf{\delta = \frac{\delta_1}{2\sin\emptyset} = \frac{\frac{Ph.\tan\emptyset}{EA.4\sin\emptyset}}{2\sin\emptyset} = \frac{Ph.\tan\emptyset}{EA.8\sin^2\emptyset}} \quad (3)$$

And, substitution δ to the equation of the rod forces:

$$\mathbf{F\sin\emptyset = \frac{EA\sin\emptyset\frac{Ph.\tan\emptyset}{EA.8\sin^2\emptyset}}{2s} = P.\sin\emptyset\frac{h.\tan\emptyset}{16s.\sin^2\emptyset}} \quad (4)$$

$$\mathbf{N = \frac{EA\frac{Ph.\tan\emptyset}{EA.8\sin^2\emptyset}}{2s} = P\frac{h.\tan\emptyset}{16s.\sin^2\emptyset}} \quad (5)$$

While, horizontal rod force (T_F):

$$\mathbf{T_F = \left(f_{yd}A_d.\sin\emptyset + f_yA_{s\prime}\right)\frac{1}{16}\frac{h.\tan\emptyset}{s.\sin^2\emptyset}} \quad (6)$$

When the skeletal moment is denoted by (M_F):

$$\mathbf{M_F = \left(f_{yd}A_d.\sin\emptyset + f_yA_{s\prime}\right)\frac{1}{16}\frac{h.\tan\emptyset}{s.\sin^2\emptyset}(d - d')} \quad (7)$$

Furthermore, the moment of anchoring BTR is denoted by (MP_F):

$$MP_F = M_n + M_F \quad (8)$$

Therefore, the empirical formula can be written as:

$$\mathbf{MP_F = A_sf_y\left(d - \frac{a}{2}\right) + \left(f_{yd}A_d.\sin\emptyset + f_yA_{s\prime}\right)\frac{1}{16}\frac{h.\tan\emptyset}{s.\sin^2\emptyset}(d - d')} \quad (9)$$

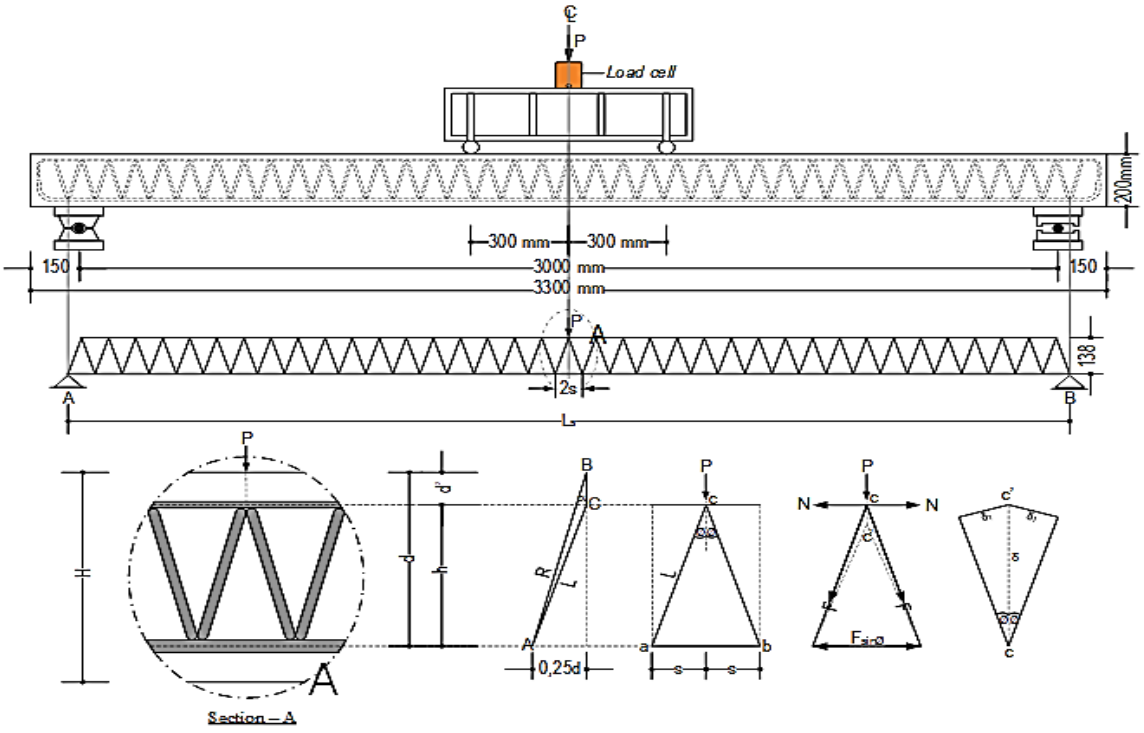

Fig. 6 Concrete beam with frame analogy

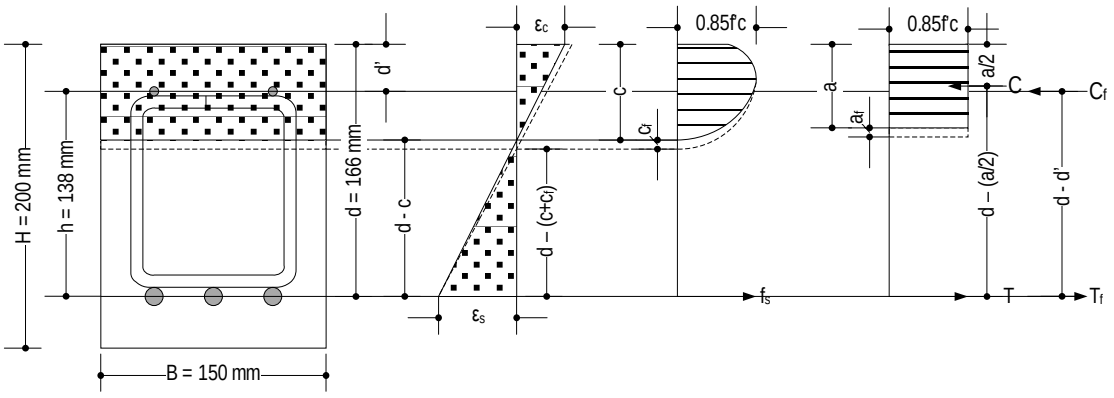

Fig. 7 Whitney voltage block

Table 3 The ratio of the moment of test results with theoretical

	Test results			Theoretical			Ratio (%)	
	P (kN)	Mn (kNm)	MP_F (kNm)	P (kN)	Mn (kNm)	MP_F (kNm)	P	Mn or MP_F
Beam BN	28.11	17.67	-	28.05	17.64	-	0.99	0.99
Beam BTR25	31.12	-	19.48	32.67	-	20.41	1.05	1.05
Beam BTR50	30.31	-	18.99	29.73	-	18.65	0.98	0.98
Beam BTR75	29.46	-	18.49	29.14	-	18.29	0.97	0.99

The theoretical moments for BN beams and BTR beams are determined by replacing the deflection load P of the test results with the equation of the bending moment where M = 0.81 + 0.60 P [19-21]. According to those mentioned in Table 3, nominal moment (Mn), and frame retaining moment (MPF) for BN and BTR beams. The calculation results show that the test results moment potential has a ratio value of 0.97 to 1.05 compared to the theoretical outcome moment or a general formula scale ratio of 0.90 to 1.0 well classified.

4. CONCLUSIONS

Subsequent conclusions are taken from the experimental test results and discussion. Increase the beam strength by 10.23 percent, the BTR50 beam by 7.47 percent, and the BTR75 beam by 4.60 percent from the BN beam as it hits the ultimate load to the flexural potential with the MPF frame retention moment on the BTR25 beam. Recommend an MPF frame retention moments empirical formula as follows: $\mathbf{MP_F = A_s f_y \left(d - \frac{a}{2}\right) + \left(f_{yd} A_d . \sin\emptyset + f_y A_{s'}\right) \frac{1}{16} \frac{h.\tan\emptyset}{s.\sin^2\emptyset} (d - d')}$.

Further research on the skeletal spatial framework and geometrical reinforcement of the sliding press collapse and building structures with complicated shapes is required.

5. REFERENCES

[1] Djamaluddin R., Bachtiar Y., Irmawati R., Akkas A. M., and Latief R. U., Effect of The Truss System to The Flexural Capacity of The External Reinforced Concrete Beams. International Journal of Civil, Structural, Construction, and Architectural Engineering, Vol. 8, Issue. 6, 2014, pp. 938-942.

[2] Saju S. M., and Usha S., Study on Flexural Strength of Truss Reinforced Concrete Beams. International Research Journal of Engineering and Technology, Vol. 3, Issue 7, 2016, pp. 1541-1545.

[3] Campione, Giuseppe, Piero Colajanni, and Alessia Monaco, Analytical Evaluation Of Steel–Concrete Composite Trussed Beam Shear Capacity. Materials and Structures, Vol. 49, Issue. 8, 2016, pp. 3159-3176.

[4] Trentadue F., Mastromarino E., Quaranta G., Petrone F., Monti G., and Marano G. C., Bending Stiffness of Truss-Reinforced Steel-Concrete Composite Beam. Open Journal of Civil Engineering, Vol. 4, Issue 3, 2014, pp. 285-300.

[5] Deshpande V. S., and Fleck N. A., Collapse of Truss Core Sandwich Beams in 3-Point Bending. International Journal of Solids and Structures, Vol. 38, Issue 36-37, 2001, pp. 6275-6305.

[6] Herman Parung, M. Wihardi Tjaronge, Rudy Djamaluddin, Study on The Efficiency Using Nature Materials in The Structural Elements of Reinforced Concrete Beam. International Conference on Engineering and Technology Development (ICETD), 2013.

[7] Herman Parung, Muhammad W. Tjaronge, and Rudy Djamaluddin, Flexural Characteristics of Reinforced Concrete Beam Using Styrofoam Filled Concrete (SFC) in Tension Zone. International Journal of Engineering and Technology, Vol. 7, Issue 1, 2015, pp. 1-7.

[8] Leopoldo Tesser and Roberto Scotta, Flexural and Shear Capacity of Composite Steel Truss and Concrete Beams with Inferior Precast Concrete Base. Engineering Structures, Vol. 49, 2013, pp. 135–145.

[9] Piero Colajanni, Lidia La Mendola, Giuseppe Mancini, Antonino Recupero, Nino Spinella, Shear Capacity in Concrete Beams Reinforced by Stirrups with Two Different Inclinations. Journal Engineering Structures, Vol. 81, 2014, pp. 444-453.

[10] Rudy Djamaluddin, Rita Irmawati, Arbain Tata, Flexural Capacity of Reinforced Concrete Beams Strengthened Using GFRP Sheet After Fatigue Loading for Sustainable Construction. Key Engineering Materials, Vol. 692, 2016, pp 66-73.

[11] Rita Irmawaty and Rudy Djamaluddin, Bending Capacity of Styrofoam Filled Concrete (SFC) Using Truss System Reinforcement. Conference for Civil Engineering Research Networks (CONCERN), Bandung, Indonesia, 2014.

[12] Pieter Lourens Frans, Herman Parung, Rudy Djamaluddin, Rita Irmawaty, The Effect of Space Bar in The Truss Reinforcing System to The Flexural Capacity of Reinforced Concrete Beams. International Journal of Civil Engineering and Technology, Vol. 10, Issue 4, 2019, pp. 754-762.

[13] Mochamad Solikin, Alfian Nur Zaini, Budi Setiawan, Ali Asroni, Flexural Strength Analysis of Styrofoam Concrete Hollow Panel Walls Incorporated with High Volume Fly Ash. Civil Engineering and Architecture, Vol. 8, Issue. 3, 2020, pp. 320 – 325.

[14] Igibah Ehizemhen C., Agashua Lucia O., Sadiq Abubakar A., Statistical Analysis and Corrosion Assessment of Nigeria Steel Rebars: Case Study South-West, Nigeria, Civil Engineering and Architecture, Vol. 7, Issue. 6, 2019, pp. 278 - 285.

[15] Pieter Lourens Frans, Herman Parung, Rudy Djamaluddin, Rita Irmawaty, Effects of Truss System Reinforcements on Flexural Behavior of Reinforced Concrete Beams, Proceedings Annual Conference on Engineering and Applied Science (ACEAT) Fukuoka, Japan, 2017.

[16] Hamkah M.W. Tjaronge R. Djamaluddin, and Nasruddin, Prediction Model of Compressive Strength of Concrete Composed of Portland Composite Cement, Marine Sand, and Sea Water Using Maturity Method, International Journal of Applied Engineering Research, Vol. 13, Issue. 3, 2018, pp. 1748-1754.

[17] Saing Z., Ibrahim M.H., and Irianto, Volume Change and Compressive Strength of Compacted Lateritic Soil under Drying-Wetting Cycle Repetition. International Journal of Geomate, Vol. 19, Issue 74, 2020, pp. 75-82.

[18] Saing Z., Ibrahim M.H., and Irianto, Experimental Investigation on Strength Improvement of Lateritic Halmahera Soil Using Quicklime Stabilization. IOP Conference Series: Earth and Environmental Science, Vol. 419, 2020, pp. 012013.

[19] Adam M. A., Said M., Mahmoud A. A., and Shanour A. S., Analytical and Experimental Flexural Behavior of Concrete Beams Reinforced with Glass Fiber Reinforced Polymers Bars. Construction and Building Materials, Vol. 84, 2015, pp. 354-366.

[20] Marí A. R., Bairán J. M., and Duarte, N, Long-Term Deflections in Cracked Reinforced Concrete Flexural Members. Engineering Structures, Vol. 32, Issue 3, 2010, pp. 829-842.

[21] Marí A. R., Oller E., Bairán J. M., and Duarte N, Simplified Method for The Calculation of Long-Term Deflections in FRP-Strengthened Reinforced Concrete Beams. Composites Part B: Engineering, Vol. 45, Issue 1, 2013, pp. 1368-1376